Research paper

The effect of sulfate species on the activity of NH$_3$-SCR over Cu/SAPO-34

Chen Wang [a], Jun Wang [a], Jianqiang Wang [a], Tie Yu [a], Meiqing Shen [a,b,c,*], Wulin Wang [a], Wei Li [d,*]

[a] Key Laboratory for Green Chemical Technology of State Education Ministry, School of Chemical Engineering & Technology, Tianjin University, Tianjin 300072, PR China
[b] Collaborative Innovation Centre of Chemical Science and Engineering (Tianjin), Tianjin 300072, PR China
[c] State Key Laboratory of Engines, Tianjin University, Tianjin 300072, PR China
[d] General Motors Global Research and Development, Chemical Sciences and Materials Systems Lab, 30500 Mound Road, Warren, MI, 48090, USA

ARTICLE INFO

ABSTRACT

The deactivation mechanism by different types of sulfate was investigated for the selective catalytic reduction of NO$_x$ on Cu/SAPO-34 catalyst. A Cu/SAPO-34 catalyst was treated with 50 ppm SO$_2$ alone at 150 and 250 °C or in the presence of a SCR feed at 250 and 350 °C. Copper sulfate was found on all sulfated catalysts, but ammonia sulfate was found only on the catalyst sulfated in the SCR feed at 250 °C. In situ DRIFTs results show that both copper sulfate and ammonia sulfate species are formed on the isolated Cu^{2+} sites. All sulfated catalysts have lower NO$_x$ conversions compared with the unsulfated catalysts due to reduced number of active sites. However, their apparent activation energies for the SCR reaction remain the same, and their turnover frequencies are identical. This suggests that the deactivation mechanism is similar regardless of the type of sulfate species. On the other hand, it was found that ammonia sulfate was easier to remove than copper sulfate by a desulfation treatment at 600 °C, resulting in a larger extent of activity recovery.

© 2016 Elsevier B.V. All rights reserved.

1. Introduction

Nitrogen oxides (NO$_x$) are one of the major air pollutants from mobile and stationary sources, and selective catalytic reduction (SCR) of NO$_x$ with NH$_3$ is the most efficient commercial technology for NO$_x$ abatement. Recently, Cu/SAPO-34, as a SCR catalyst for diesel vehicles, has been investigated by many researchers because of its excellent NH$_3$-SCR activity, good thermal stability and low N$_2$O formation [1–5].

However, catalyst poisoning by sulfur has been recognized as a potential issue for its practical application. Sulfur oxides are known to be a deactivation species for SCR catalysts [6,7]. The poisoning effect of SO$_2$ without NH$_3$ on Cu/SAPO-34 has been studied by many groups and the deactivation is due to the formation of sulfate species on the isolated Cu^{2+} ions (active sites). For example, our earlier study [8] showed that the higher the SO$_2$ concentration and the longer the exposure time, the more of copper sulfate formation and therefore the lower the NO$_x$ conversion. Brookshear [9] found that

more sulfate was formed at 400 °C than at 250 °C on a Cu/SAPO-34 catalyst with a feed containing 500 ppm SO$_2$, resulting in more decrease in NO$_x$ conversion. Wijayanti [10] further found that sulfated Cu/SAPO-34 had less available copper sites, which is the main reason for catalyst deactivation. In real application process, the catalysts usually go through SO$_2$-containing streams in the presence of ammonia, which cause ammonium sulfate formation [11,12]. Ham [13,14] reported that ammonium sulfate formed on a Cu/mordenite catalyst blocked the zeolite pores and significantly decreased its surface area. As a result, the NO$_x$ conversion decreased. Zhang [15] preliminary found that the NO$_x$ conversion reducing on Cu/SAPO-34 at low temperature involved the formation of ammonium sulfate species when SO$_2$ existed in SCR feed, which may result in both active sites poisoning and the pores blocking. The poisoning mechanism by ammonia sulfate species on Cu/SAPO-34 (which factor, active sites poisoning or pores blocking or both, determines NO$_x$ conversion reducing under various sulfate species?), however, was not clearly substantiated. Moreover, to the best of our knowledge, there were no published studies that examine the detailed locations of the ammonia sulfate species formed on Cu/SAPO-34 and the effect of ammonia sulfate species on isolated Cu^{2+} ions. In addition, what is not clear is the difference in poisoning mechanism by different types of sulfate species, i.e. ammonia sulfate vs. copper

* Corresponding authors at: School of Chemical Engineering and Technology, Tianjin University, 92 Weijin Road, Nankai District, Tianjin 300072, China.
E-mail addresses: mqshen@tju.edu.cn (M. Shen), wei.1.li@gm.com (W. Li).

sulfate. How do they coordinate with the active sites, what are the necessary conditions for their formation and removal, what is the role of NH_3 plays in copper sulfate formation?

In this paper, the effect of sulfation on Cu/SAPO-34 catalysts as a function of sulfation temperature and feed composition is reported to identify the necessary conditions to form Cu sulfate and NH_3 sulfate species. By using a number of characterization tools (TGA, TPD, in situ DRIFTs and EPR) in combination with the kinetic studies, we intend to answer the question, how Cu/SAPO-34 is poisoned by sulfate species.

2. Experimental

2.1. Catalyst preparation

Cu/SAPO-34 catalysts were synthesized using the 'one-pot' method [16]. The synthesis gel consists of 1 Al_2O_3, 0.9 P_2O_5, 0.7 SiO_2, 0-0.2 CuO, 2 Morpholine (MOR), 0-0.2 Tetraethylenepentamine (TEPA) and 5.69H_2O (molar basis). The material sources for Si, P, Al, and Cu are silica sol (40 wt% SiO_2), orthophosphoric acid (85 wt% H_3PO_4), pseudoboehmite (68 wt% Al_2O_3), and Copper (II) sulfate pentahydrate (purity above 99 wt%), respectively. MOR (purity 99 wt%) was used as the templating agent and TEPA (purity 90 wt%) as complexing agent for copper (II). The resulting gel was sealed in a 200 ml Teflon-lined stainless steel pressure vessel and heated in an oven at 200 °C under autogenic pressure for 48 h. After the crystallization process, the sediment was separated from the mother liquid via centrifugation, washed by distilled water and then filtrated. Finally, the power was dried at 120 °C in oven for 12 h and calcined in muffle furnace with air at 650 °C for 6 h.

2.2. Sulfation treatment

The resulting sample was hydrothermally aged with 10% H_2O in air at 750 °C for 4 h and is named as fresh Cu/SAPO-34 (F-Cu).

The catalysts were sulfated with SO_2-containing streams, in the presence or absence of ammonia. For NH_3-free sulfation, the catalyst was sulfated at 150 and 250 °C with a feed containing 50 ppm SO_2, 500 ppm NO, 7% CO_2, 5% H_2O in air. For sulfation with both SO_2 and NH_3, the sulfation was conducted at 250 and 350 °C with a feed containing 50 ppm SO_2, 500 ppm NH_3, 500 ppm NO, 7% CO_2, 5% H_2O in air. In both cases, the sulfation lasted for 16 h with a total sulfur throughput of 68.6 mg SO_2/g catalyst. A detailed description of sulfation conditions and their corresponding catalyst nomenclatures are shown in Table 1. The sulfated catalysts are denoted as 'S-N (if used)-Cu-T', where S stands for SO_2, N for NH_3 and T for sulfation temperature. For comparison, the SAPO-34 support was also treated with a feed containing both NH_3 and SO_2 at 250 °C, denoted as 'S-N-SAPO-250'. After sulfation, a desulfation treatment were carried out over all samples at 600 °C with 5% O_2/N_2 for 0.5 h.

2.3. Catalyst characterization

The XRD spectra was collected using X' Pert Pro diffractometer operating at 40 kV and 40 mA with nickel-filtered Cu Kα radiation (λ=1.5418 Å). The data were collected in the 2θ range between 5 and 50° with a step size of 0.01°.

BET surface areas were measured by N_2 adsorption-desorption at −196 °C using an automatic micropore physisorption analyzer after degassing samples at 150 °C for at least 5 h under 0.133 Pa pressure.

The following experiments, TGA, TPD, in situ DRIFTs and EPR, were performed to identify the sulfate species and its location. Notably, S-N-Cu-250 and S-N-Cu-350 were sulfated with both SO_2 and NH_3. NH_3 adsorbed on acid sites (Brønsted and Lewis acid sites) has impact on identification and analysis of ammonia sulfate

species, so NH_3 adsorbed on acid sites should be eliminated before our testing. We have done an experiment on F-Cu to justify that $NO+O_2$ treatment is a reliable method to consume all adsorbed NH_3 on acid sites. F-Cu was pre-adsorbed NH_3 at 250 °C. This NH_3 loaded F-Cu catalyst was then treated with a feed containing 500 ppm NO_x and 5% O_2 at the same temperature until the outlet NO_x concentration reaching to a stable level. A TPD experiment was conducted on this NH_3 loaded F-Cu catalyst from 250 °C to 600 °C at a rate of 10 °C/min in 500 ml/min N_2, but no NH_3 desorption was detected. Based on the results, the catalyst, S-N-Cu-250 or S-N-Cu-350, was first purged with a feed containing 500 ppm NO_x and 5% O_2 at 250 °C. After the NO_x concentration returned to 500 ppm, the catalyst was purged with N_2 for 1 h at the same temperature. Then, the temperature was cooled to room temperature in N_2. The catalysts was then ready for characterizations.

The thermal gravimetric experiments were conducted on MET-TLER TOLEDO thermal gravimetric analyzer (TGA). A 15 mg sample was first heated from room temperature to 150 °C at 10 °C/min in a gas flow containing N_2 (47.5 ml/min) and O_2 (2.5 ml/min) and kept at 150 °C for 30 min. The temperature was then increased from 150 to 800 °C at a rate of 10 °C/min in the same gas stream.

The temperature-programmed desorption (TPD) experiments were performed to evaluate the desorption/decomposition profiles of sulfate species. A catalyst was first pre-treated at 250 °C for 30 min in 5% O_2/N_2 and then cooled to 100 °C in N_2. For TPD experiments, the temperature increased from 100 to 600 °C at a rate of 10 °C/min in N_2 (500 ml/min). The exiting gases, SO_2 and NH_3, were analyzed by FTIR (MKS-2030).

In situ diffuse reflectance infrared Fourier transform spectra (Nicolet 6700 spectrometer) was used to monitor the formation of copper sulfate and ammonia sulfate species during the process of exposing a catalyst to the SO_2 feed (43 ppm SO_2 and 20% O_2 in N_2) and the SO_2/NH_3 feed (43 ppm SO_2, 500 ppm NH_3 and 20% O_2 in N_2) at 250 °C, respectively. Before each measurement, a fresh Cu/SAPO-34 sample was dried at 250 °C for 30 min. In order to minimize the interference of water with IR spectra, all the DRIFTs data were collected in the absence of water. The titration experiment with $NO+O_2$ was also performed after the catalyst sulfated with both SO_2 and NH_3. The DRIFT spectra were recorded in the range of 4000 to 650 cm^{-1} with a resolution of 4 cm^{-1}. Nicolet OMNIC software was used to convert absorbance to Kubelka-Munk (K-M) units. To determine the effect of support sulfation, the same process on H/SAPO-34 was performed using in situ DRIFTs.

The electron paramagnetic resonance (EPR) spectra were recorded using a Bruker ESP320 spectrometer, and Bruker ESP320E software was used for data analysis. Prior to the EPR measurement, a Cu/SAPO-34 sample was treated in 20% O_2/N_2 at 250 °C for 2 h. X-band (ν=9.78 GHz) spectra were recorded at room temperature with the magnetic field sweeping from 2000 to 4000 Gauss. The content of isolated Cu^{2+} was calculated from double integration of the EPR spectra. The calibration curve was obtained from the EPR results of reference copper sulfate solutions at various concentrations. All the EPR spectra were obtained at −150 °C.

2.4. SCR activity and kinetics test

The SCR activity was measured in a quartz tube reactor using 0.1 g catalyst mixed with 0.9 g quartz sand. The catalyst bed was positioned in the tube with quartz wool on both sides. The temperature was controlled by a YUDIAN 808P controller with a K-type thermocouple. The feed gases were controlled by Beijing Metron S49–33 M/MT mass flow controllers. FTIR (MKS 2030) was used to measure the concentrations of NO, NO_2, N_2O and NH_3. The total gas flow rate for all experiments was controlled at 1000 ml/min

Table 1
Sulfation conditions and BET surface areas.

Catalysts	Poisoned conditions	Surface Area (m^2/g)
F-Cu	–	360
S-Cu-150	50 ppm SO_2 at 150 °C for 16 h	334
S-Cu-250	50 ppm SO_2 at 250 °C for 16 h	330
S-N-Cu-250	50 ppm SO_2, 500 ppm NH_3 at 250 °C for 16 h	280
S-N-Cu-350	50 ppm SO_2, 500 ppm NH_3 at 350 °C for 16 h	332
S-N-SAPO-250	50 ppm SO_2, 500 ppm NH_3 at 250 °C for 16 h	–

Base feed: 500 ppm NO_x, 7% CO_2 and 5% H_2O in air. Total flow rate: 1000 ml/min.

(GHSV = 72, 000 h^{-1}). Prior to the SCR experiment, a catalyst was heated up to 250 °C and kept at this temperature for 30 min under a flow of 5% O_2 in N_2. The reaction feed gas consists of 500 ppm NO_x, 500 ppm NH_3 and 5% O_2, 7%CO_2, 3% H_2O and balance N_2. Steady-state NO_x conversions were measured between 100 and 600 °C at a 50 °C interval. Data were continuously collected after the system has been stabilized for at least 1 h at each temperature. The NO_x conversion is calculated based on Eq. (1).

$$NO_X \, Conversion \, (\%) = \frac{NO_{xinlet} - NO_{xoutlet}}{NO_{xinlet}} \times 100\% \quad (1)$$

Where $NO_x = NO + NO_2$

For tests used for reaction rate measurement, 25 mg catalyst was used and mixed with 125 mg quartz sand (GHSV = 432, 000 h^{-1}), which ensures that the reaction system is free of external diffusion control (see Fig. S1a in Supporting information for details). To minimize internal diffusion control, catalyst particles between 80 and 100 mesh were selected (see Fig. S1b in Supporting information for details). For kinetic tests, a sample was pre-treated in the same way as for activity measurement, but the conversion was measured in the absence of H_2O and CO_2 because the presence of H_2O and CO_2 had weak effect on SCR activity over Cu/SAPO-34 especially at low temperature based on our previous work [2]. The steady-state NO_x conversions were controlled below 20% and were collected at a temperature interval of 20 °C (see Fig. S1c in Supporting information for details), The NH_3-SCR reaction rates are calculated based on Eq. (2).

$$Rate \left[mol_{NO_x} \cdot g_{catal} \cdot S^{-1} \right]$$
$$= \frac{X_{NO_X} \, [\%] \times F_{NO_X} \left[l_{NO_x} \cdot min^{-1} \right]}{m_{catal} \, [g] \times 60 \left[s \cdot min^{-1} \right] \times 22.4 \left[L \cdot mol^{-1} \right] \times 100} \quad (2)$$

Where X_{NO_X} is NO_x conversion, F_{NO_X} is volumetric flow rate of NO_x, m_{catal} is catalyst weight.

Turnover frequency (TOF) is calculated based on Eq. (3).

$$TOF \left[s^{-1} \right]$$
$$= \frac{X_{NO_X} \, [\%] \times F_{NO_X} \left[L_{NO_x} \cdot min^{-1} \right]}{60 \left[s \cdot min^{-1} \right] \times 22.4 \left[L \cdot mol^{-1} \right] \times 100 \times [number \, of \, Active \, Sites] \, [mol]} \quad (3)$$

Where X_{NO_X} is NO_x conversion, F_{NO_X} is volumetric flow rate of NO_x, [Number of active sites] is the amount of isolated Cu^{2+} sites measured by EPR.

3. Results

3.1. XRD and BET results

To examine the impact of sulfation on the structure of Cu/SAPO-34 catalyst, XRD experiments were performed. As shown in Fig. S2, all the samples have the typical chabazite structure [17] with similar crystallinities.
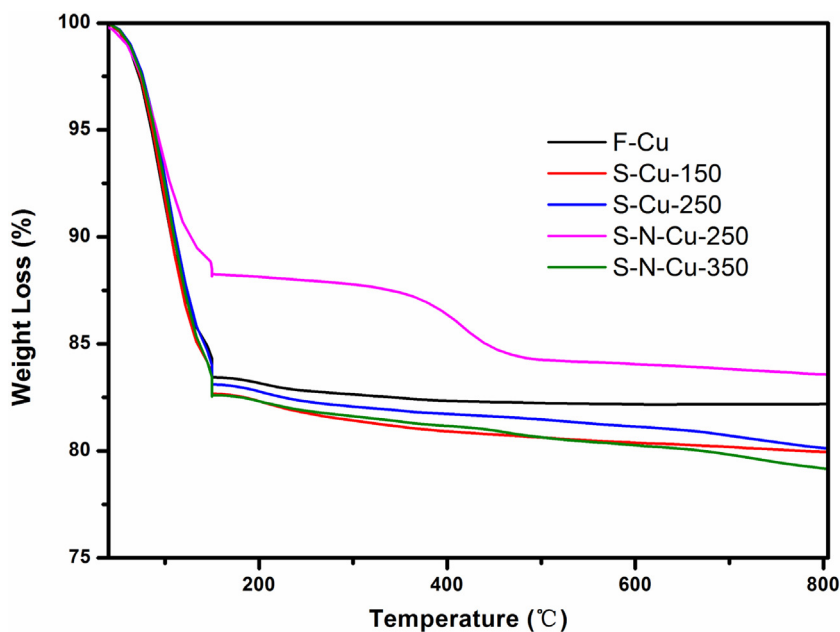
Fig. 1. TGA data of fresh and sulfated samples.

Table 1 compares the BET surface areas of the sulfated samples under different sulfation conditions. A 20% reduction in surface area was found on S-N-Cu-250 relative to the fresh catalyst and a 10% reduction on the rest of sulfated samples.

3.2. TGA measurements

Fig. 1 compares the TGA profiles of the fresh Cu/SAPO-34 catalyst with those of sulfated catalysts. Sample weight loss was found in three temperature regimes. The first weight loss occurred below 200 °C, which can be attributed to water evaporation [18]. The second weight loss was found between 300 and 500 °C, and the weight loss decreases in the order: S-N-Cu-250 (3.5 wt%) > S-N-Cu-350 (1.0 wt%) > S-Cu-250 (0.9 wt%) > S-Cu-150 (0.8 wt%). The third weight loss was observed between 500 and 800 °C, which decreases in the following order: S-N-Cu-350 (1.4 wt%) > S-Cu-250 (1.3 wt%) > S-N-Cu-250 (0.7 wt%) > S-Cu-150 (0.6 wt%).

3.3. TPD measurements

Fig. 2 shows the TPD profiles of four sulfated catalysts. For catalysts sulfated with the SO_2/NH_3 feed, a $NO+O_2$ titration treatment was performed to selectively remove the NH_3 adsorbed on the acid sites. Thus, the NH_3 evolution during the TPD experiment can be associated with a sulfate species (Fig. S5) and here we assign this sulfate species as ammonia sulfate species rather than ammonium sulfate species because there is not any NH_4^+ left on sulfated sample (will be further discussed in Section 4.2).

As shown in Fig. 2a, on S-Cu-150 and S-Cu-250, only SO_2 peak was found above 300 °C (centered around 500 °C). On S-N-Cu-250, however, an NH_3 peak was observed between 300 and 500 °C (centered around 370 °C) and a broad SO_2 peak above 300 °C (centered around 400 °C) (Fig. 2b). On S-N-Cu-350, only one SO_2 peak was found centered at 500 °C, which is similar to those of S-Cu-150 and S-Cu-250 (Fig. 2c).

3.4. In situ in situ DRIFTs

In situ DRIFTs experiments were performed to identify the surface species formed on Cu/SAPO-34 during a sulfation treatment and their corresponding sites. Fig. 3 shows the DRIFTs spectra of Cu/SAPO-34, which was exposed to two different sulfur-containing feed conditions at 250 °C. The bands around 3624 and 3598 cm^{-1} are assigned to the Brønsted OH groups as (Si-(OH)-Al) [8,18,21–23], and the negative bands at 3624 and 3598 cm^{-1} are assigned to Brønsted OH groups broken or NH_3 adsorbed on Brønsted acid sites (Si-OH-Al). The bands at 1620 cm^{-1} is assigned to adsorbed NH_3 bound to Lewis acid sites [15]. In our study, NH_3 adsorbed on Lewis acid sites (1620 cm^{-1}) come from ammonia sulfate species because the sulfated sample were treated with $NO+O_2$. Several bands centered at 1320, 1304, 1287 and 1226 cm^{-1} are ascribed to S=O and S-O vibration in sulfate on catalyst [15,19]. The bands around 885 and 854 cm^{-1} are associated with the internal asymmetric framework vibrations perturbed by isolated Cu^{2+} ions on Cu/SAPO-34 [20], and the negative bands at these locations are thus due to the occupation of the isolated Cu^{2+} cations by adsorbates.

Firstly, the sulfur poisoning over H/SAPO-34 and Cu/SAPO-34 (Fig. 3a) had no impact on Brønsted acid sites (Si-OH-Al). As shown in Fig. 3b, after the SO_2-only treatment sulfate species was formed on the isolated Cu^{2+} ions (1304 cm^{-1}). However, after the Cu/SAPO-34 catalyst was treated with the NH_3/SO_2 feed, different types of sulfate species were observed at 1320, 1287 and 1226 cm^{-1} with much higher intensities. In addition, higher intensities of negative bands at 885 and 854 cm^{-1} were observed on the NH_3/SO_2 treated Cu/SAPO-34 catalyst. Since the catalyst was further titrated with
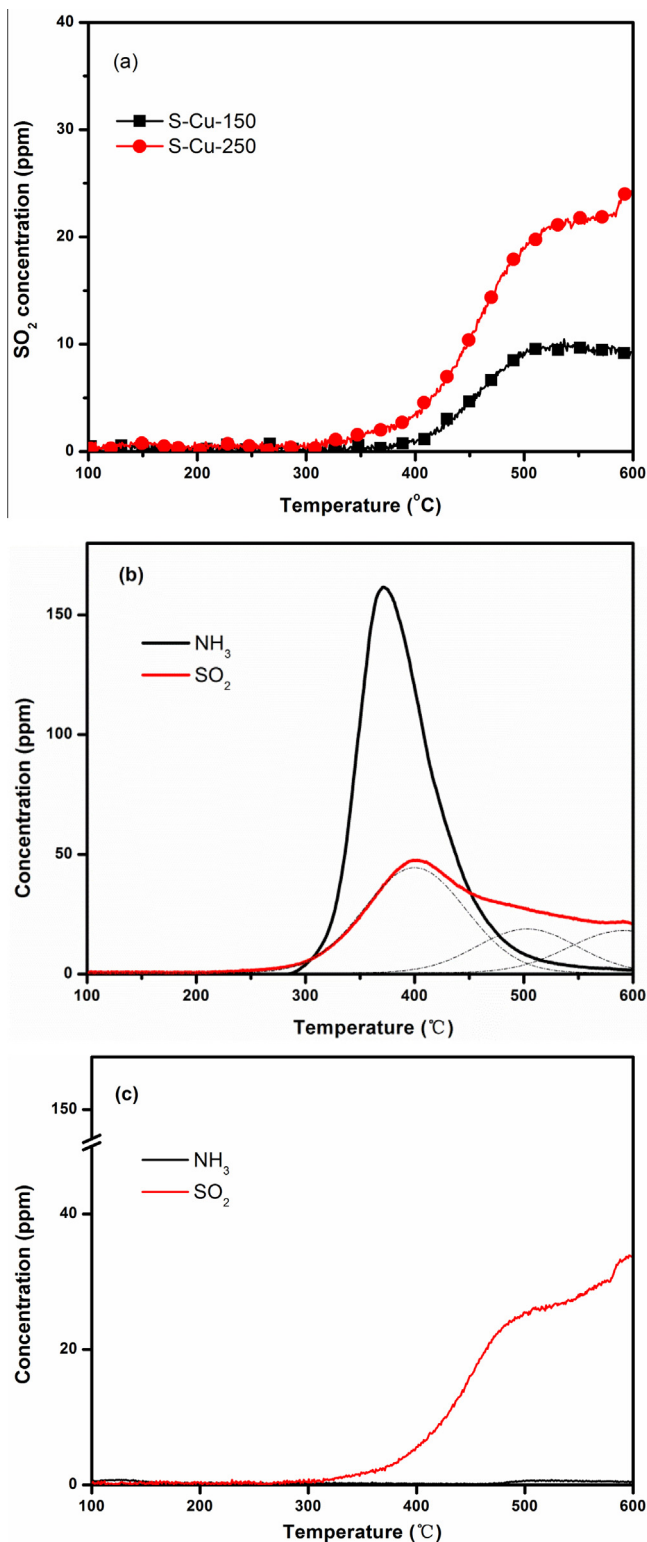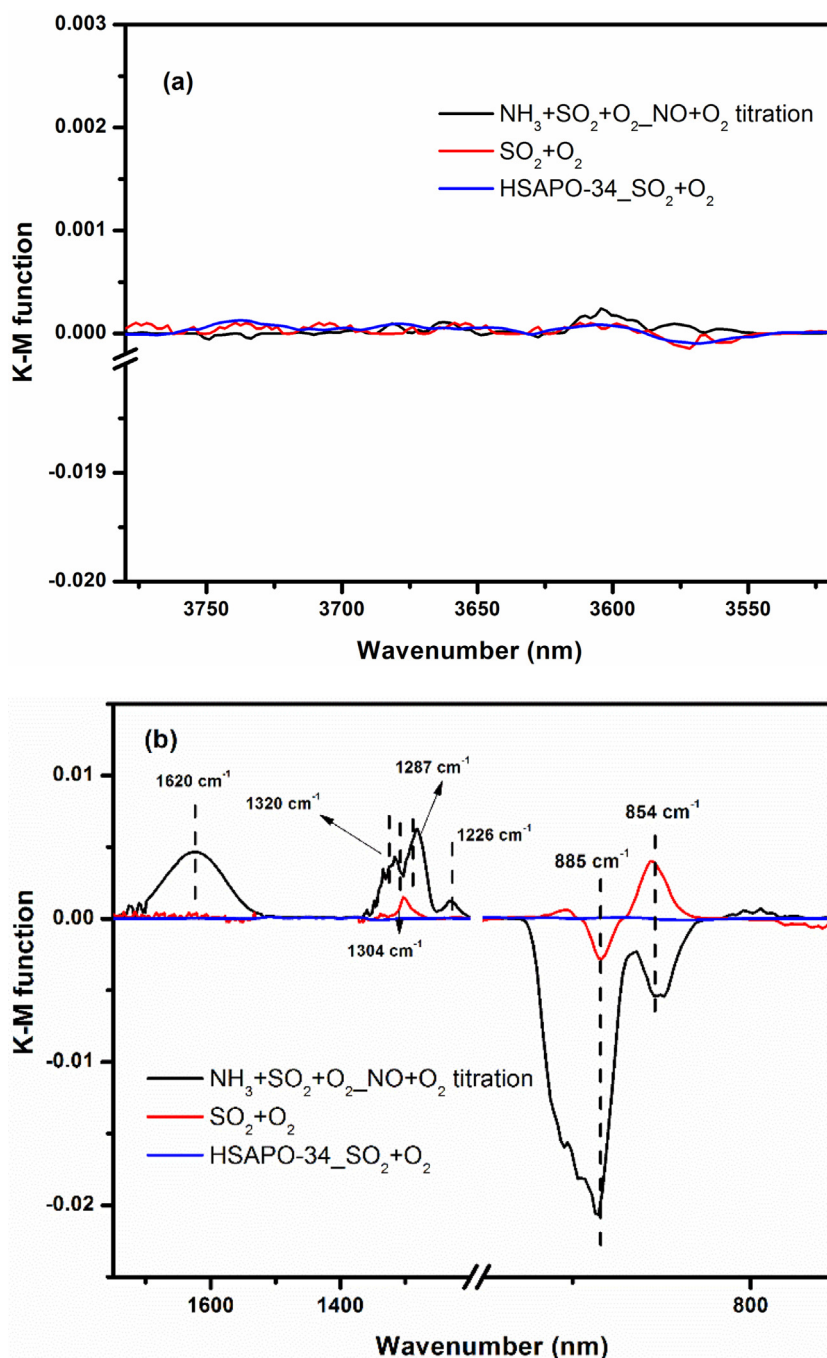

Fig. 2. TPD profiles of S-Cu-150 and S-Cu-250 (a), TPD profiles of S-N-Cu-250 after $NO + O_2$ titration (b), TPD profiles of S-N-Cu-350 after $NO+O_2$ titration (c).

NO/O_2 after the NH_3/SO_2 treatment, the NH_3 molecules adsorbed on the Brønsted acid sites should have been completely removed, leaving only those adsorbed on the isolated Cu^{2+} sites (1620 cm^{-1}).

Fig. 3. DRIFT spectra for the surface states. Black: NO+O$_2$ titration after exposure to 43 ppm SO$_2$, 500 ppm NH$_3$ and 20% O$_2$ in N$_2$ at 250 °C on Cu/SAPO-34; Red: exposing to 43 ppm SO$_2$ and 20% O$_2$ in N$_2$ at 250 °C till saturation on Cu/SAPO-34; Blue: exposing to 43 ppm SO$_2$ and 20% O$_2$ in N$_2$ at 250 °C till saturation on H/SAPO-34.

3.5. EPR results

Fig. 4 shows the EPR spectra of the Cu/SAPO-34 catalyst sulfated under different conditions. The EPR spectra show that the Cu^{2+} species of the sulfated catalysts have the same coordination environment as that of the non-sulfated catalyst (F-Cu) with g$_{//}$ = 2.39 and A$_{//}$ = 141. This suggests that the locations of the isolated Cu^{2+} ions that are not yet poisoned by sulfur remain the same. Fig. 5 compares the number of isolated Cu^{2+} ions on the sulfated Cu/SAPO-34 catalysts measured by EPR. The number of isolated Cu^{2+} ions decreases in the following order: F-Cu > S-Cu-150 > S-Cu-250 > S-N-Cu-350 > S-N-Cu-250.

3.6. Catalyst activity

To understand how sulfur poisoning affecting the catalytic activity, the NH$_3$-SCR reaction was carried out, and the results are shown in Fig. 6. Comparing to F-Cu, the NO$_x$ conversions of the sulfated catalysts decrease significantly between 100 and 400 °C but change little above 400 °C. S-N-Cu-250 is the least active catalyst below 300 °C; however, above 330 °C its activity increases more steeply relative to other sulfated catalysts. The highest N$_2$O formation is found on the unsulfated catalysts at 600 °C (7 ppm), and the sulfation treatment decrease the N$_2$O formation by 1 to 2 ppm (Fig. 6b).
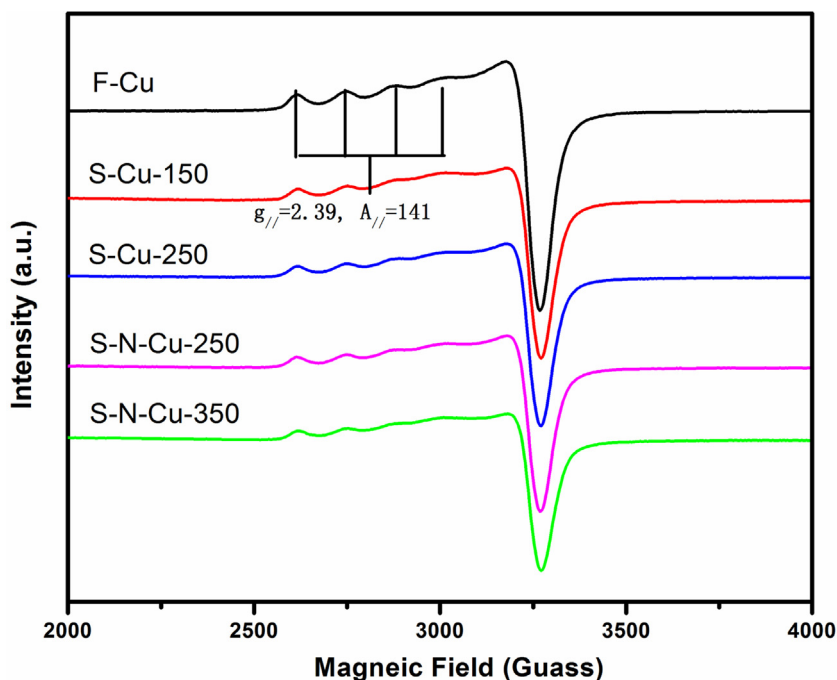
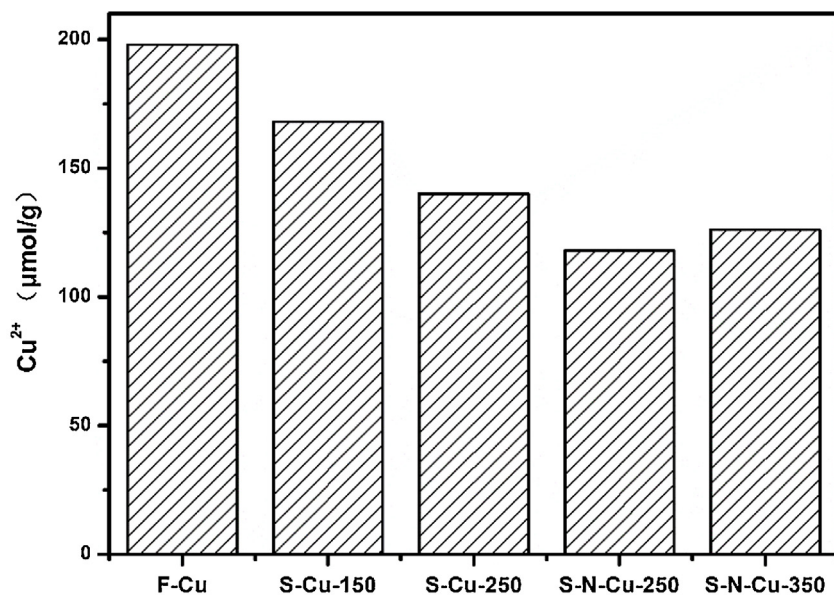**Fig. 4.** EPR spectra of Cu/SAPO-34 catalyst at −150 °C and atmospheric pressure (101.325 kPa).

Fig. 5. The amount of isolated Cu^{2+} ions in Cu/SAPO-34 catalysts estimated based on the EPR spectra.

A desulfation treatment was carried out over the sulfated catalysts at 600 °C with 5% O_2/N_2 for 0.5 h in an attempt to recover the activity suppressed by the sulfates. Fig. 7 shows the activity results of the desulfated catalysts. The NO_x conversions between 100 and 400 °C are partially recovered, among which S-N-Cu-250 recover the most (Fig. 7a). The N_2O formation of the desulfated catalysts is similar to that of the sulfated samples (Fig. 7b).

3.7. Kinetics study

Fig. 8 shows the Arrhenius plots for the SCR reaction over the fresh and sulfated catalysts. The apparent activation energies (Ea) are similar for all the catalysts, ∼20 kJ/mol. Based on Arrhenius Equation, the only parameter left that can contribute to the differ-

ence in the rate constant must be the pre-exponential factor, which decreases in the following order: F-Cu > S-Cu-150 > S-Cu-250 > S-N-Cu-350 > S-N-Cu-250.

4. Discussion

4.1. The formation of copper sulfate species and its impact on catalytic activity

Our TPD results of S-Cu-150, S-Cu-250 and S-N-Cu-350 show SO_2 evolution above 500 °C (Fig. 2a and c), which suggests that copper sulfate may be formed on these catalysts. This assumption is confirmed by the DRIFTs results (Fig. 3a), which show the presence of adsorbed sulfate species on the sulfated catalysts (1304 cm^{-1}),
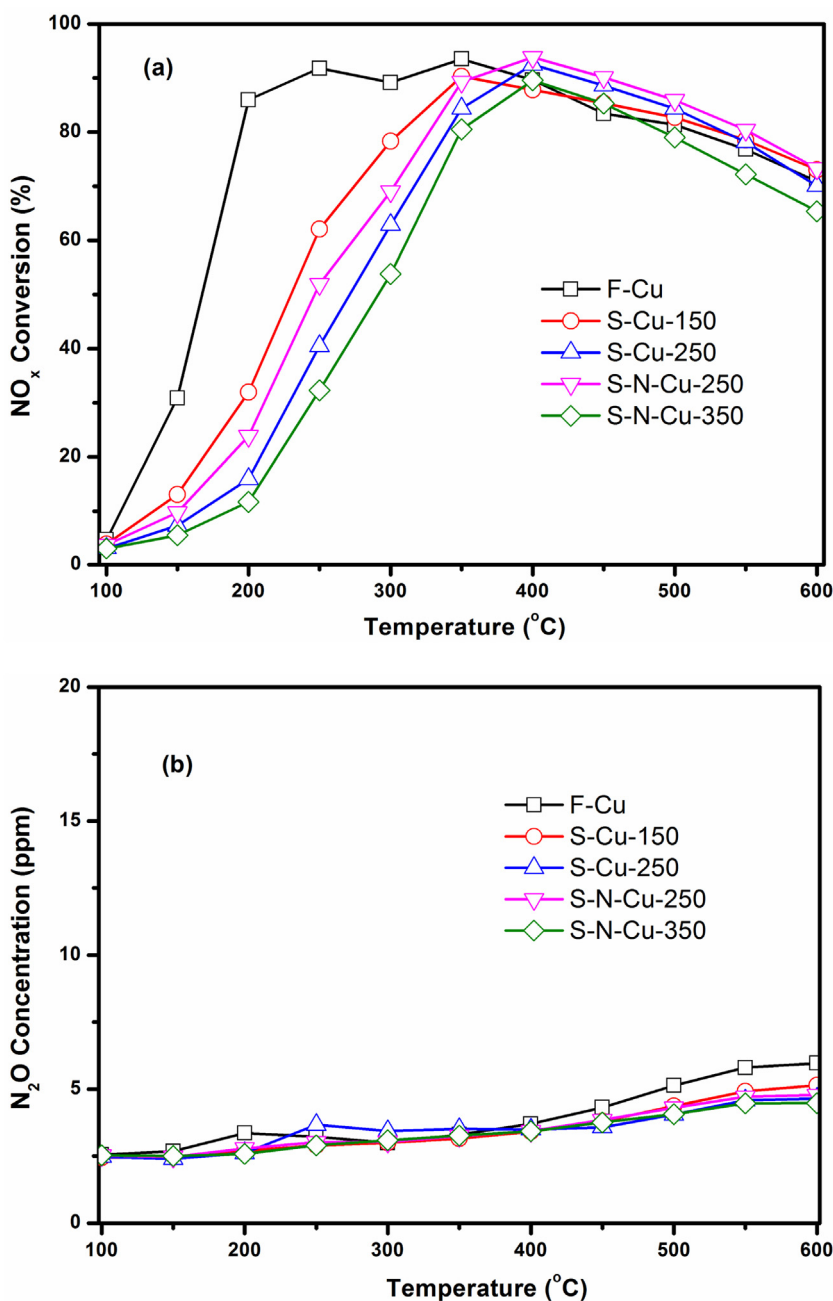
Fig. 6. NO$_x$ conversion as a function of reaction temperature over sulfated catalysts (a), N$_2$O formation during NH$_3$-SCR reaction on the sulfated catalysts (b). The reaction was carried out with a feed containing 500 ppm NO, 500 ppm NH$_3$, 5% O$_2$, 7% CO$_2$, 3% H$_2$O, balance N$_2$ and with GHSV = 72000 h^{-1}.

and this sulfate species is identified as the sulfate adsorbed on the isolated Cu^{2+} sites, as evidenced by the formation of the negative band at 885 cm^{-1} [20]. The formation of copper sulfate on the sulfated catalysts is further confirmed by the our TGA results (Fig. 1); both the sulfated catalysts and a reference copper sulfate compound (copper sulfate pentahydrate) share a similar DTG temperature range (600–800 °C) (Figs. S3 and S4). The TGA and TPD results clearly demonstrate that sulfation temperature plays an important role in copper sulfate formation; more sulfate was formed at 350 °C than at 150 or 250 °C (Figs. Fig. 1 and 2 a). On the other hand, the composition of the sulfation feed is a critical factor in determining the type of sulfate species. On S-N-Cu-250 (a sample treated with both NH$_3$ and SO$_2$ at 250 °C), in addition to copper sulfate, NH$_3$ sulfate is the dominant sulfate species, which will be further discussed in Section 4.2.

The catalytic activity of Cu/SAPO-34 is related to the amount of isolated Cu^{2+} ions, the acid concentration and the structure stability [2,16]. SO$_2$ treatment has no impact on the SAPO-34 structure as evidenced by the XRD and DRIFTS results. Moreover, the NH$_3$-TPD results (Fig. S6) show that the acid contents of the sulfated catalysts are similar to that of Cu-F. Thus, it is reasonable to believe that the activity decrease by SO$_2$ poisoning must be the result of the reduced number of the isolated Cu^{2+} sites. The extent of the decrease in isolated Cu^{2+} sites, as measured by EPR spectroscopy, is 16% and 10% as the sulfation temperature increases from 150 to 250 °C and 250 to 350 °C, respectively (Fig. 5). The kinetic experiments show that the apparent activation energies obtained on the sulfated catalysts
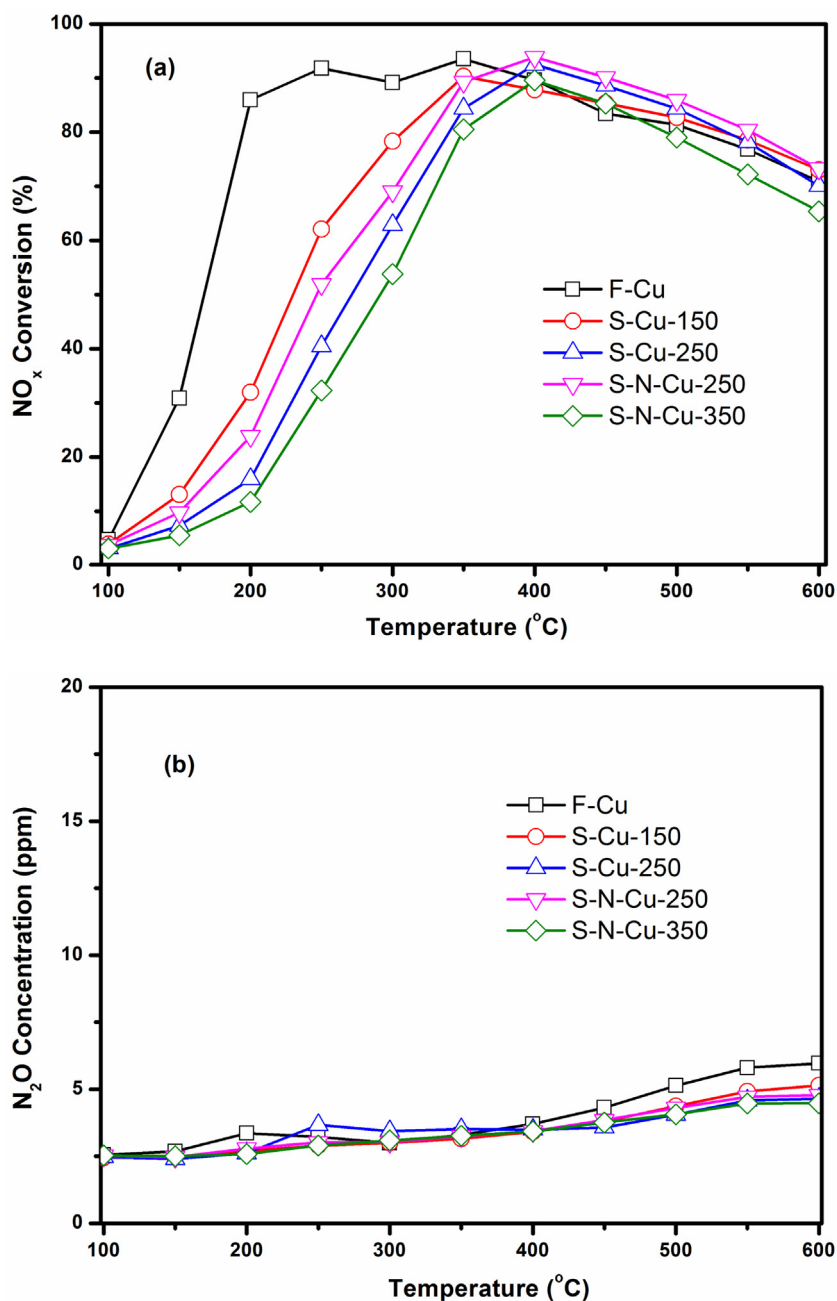
Fig. 7. NO$_x$ conversion after desulfation at 600 °C (a), N$_2$O formation during NH$_3$-SCR reaction after desulfation at 600 °C (b). The reaction was carried out with a feed containing 500 ppm NO, 500 ppm NH$_3$, 5% O$_2$, 7% CO$_2$, 3% H$_2$O, balance N$_2$ and with GHSV = 72000 h^{-1}.

are the same (see detailed calculation in Table S1). Therefore, the turnover frequencies (TOFs), calculated based on the isolated Cu^{2+} ions measured by EPR, are identical for F-Cu, S-Cu-150, S-Cu-250 and S-N-Cu-350 (Fig. 9). This clearly demonstrates that the nature of SO$_2$ poisoning is to reduce the number of isolated Cu^{2+} sites, and the sites not occupied by sulfur have the same specific rate (TOF) for the SCR reaction. As a further proof of this conclusion, we have correlated the reduced number of Cu^{2+} sites with the amount of sulfur on sulfated samples in Fig. 10. The reduced number of Cu^{2+} sites is obtained from the EPR results (Fig. 5) using F-Cu as a reference, and the amount of sulfur deposited on a sulfated catalyst can be calculated based on the TGA results (see the calculation in Supporting information for details). The calculation shows that the

reduced number of Cu^{2+} sites is directly correlated to the amount of sulfur deposited.

4.2. The formation of ammonia sulfate species and its impact on catalytic activity

The types of sulfur species formed on S-N-Cu-250 are elucidated by the TPD experiments (Fig. 2b). Because the NH$_3$ adsorbed on acid sites had already been removed prior to the TPD experiment, the simultaneous desorption of NH$_3$ and SO$_2$ around 400 °C, with integrated NH$_3$/SO$_2$ molar ratio ~2:1 (detailed calculation can be seen in Fig. S7), must be the result of NH$_3$ sulfate decomposition. The conclusion is confirmed by the DRIFTS results. No NH$_4^+$ adsorption on Brønsted acid sites was detected after NO+O$_2$ titra-
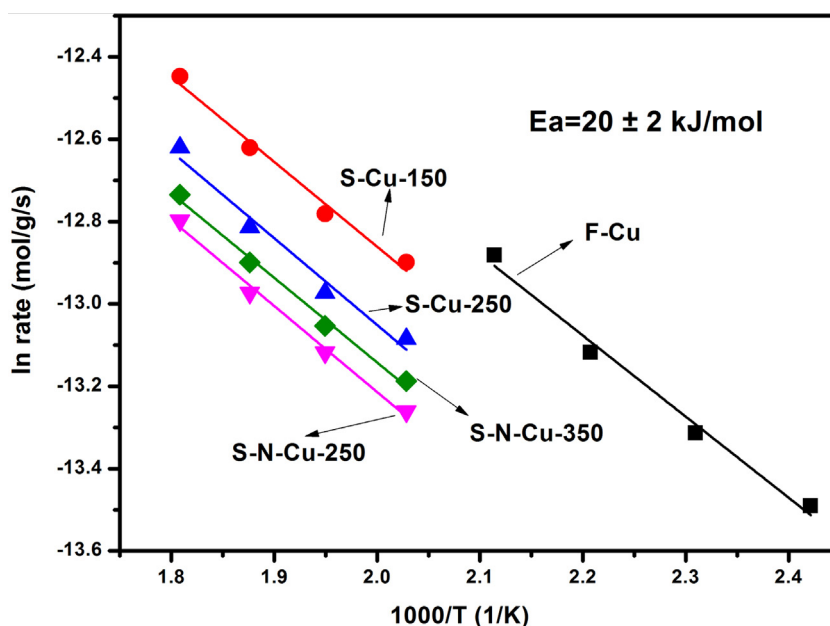
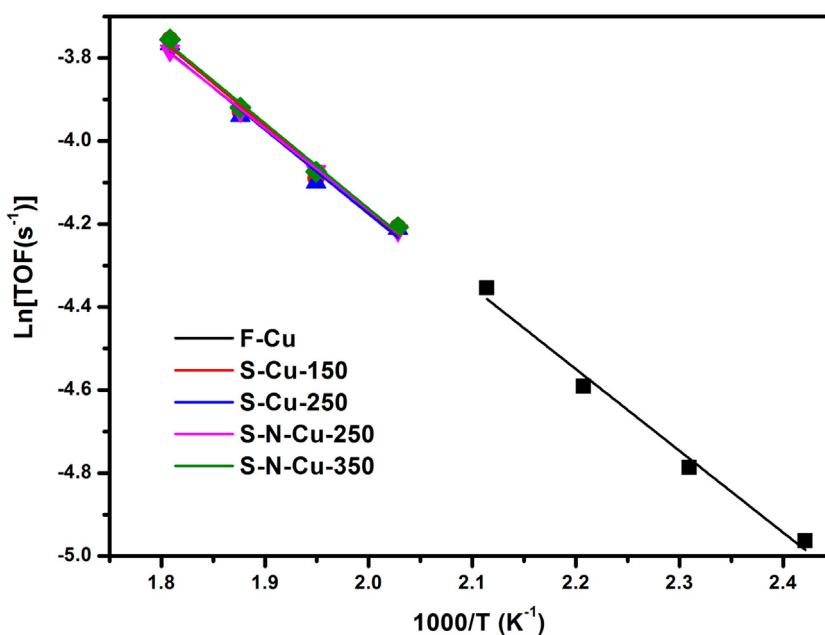**Fig. 8.** Arrhenius plots of the SCR reaction rates over fresh and sulfated samples.

Fig. 9. TOFs results over sulfated catalysts.

tion (Fig. 3), and the NH_3 species observed at $1620 \, cm^{-1}$ remained on the sulfated Cu/SAPO-34 catalyst. This suggests that this NH_3 species adsorbed on Lewis acid site is inactive for SCR and stably bonded with the sulfate species on S-N-Cu-250, which is evidenced by the formation of the band at 1320, 1287 and $1226 \, cm^{-1}$. Combining with the integrated NH_3/SO_2 molar ratio is 2 (Fig. S7), the ammonia sulfate species may be in the form of $Cu-2(NH_3)-SO_4$. In addition to the NH_3 sulfate species, copper sulfate was also found on S-N-Cu-250. The SO_2 desorption at higher temperatures (>500 °C) can only be the result of decomposition of copper sulfate since NH_3 had been gone before reaching 500 °C; the formation of copper sulfate on S-N-Cu-250 is also confirmed by the DRIFTs results (bands at 1320, 1287 and $1226 \, cm^{-1}$, and negative bands at 885 and $854 \, cm^{-1}$).

It appears that the formation of ammonia sulfate species on the catalyst is more favorable comparing to copper sulfate when a Cu/SAPO-34 catalyst is treated with an NH_3/SO_2 feed at 250 °C. Kinetically, the high concentration of NH_3 (500 ppm) would favor the adsorption of NH_3 over SO_2 on the Cu^{2+} sites, resulting ammonia sulfate species. The TGA and TPD data show that ammonia sulfate species is the dominate sulfate species; its formation may inhibit the formation of copper sulfate though not totally prevent it. Temperature is proved to be critical for ammonia sulfate species formation. At 350 °C, little ammonia sulfate species was formed when treated with the same feed (see Fig. 2c). This is because at 350 °C NH_3 adsorption is too weak and cannot compete with SO_2.

The EPR results and kinetic tests clearly demonstrate that the decrease of catalytic activity over S-N-Cu-250 is also quantitatively related to the reduction of the isolated Cu^{2+} sites. Consequently, the
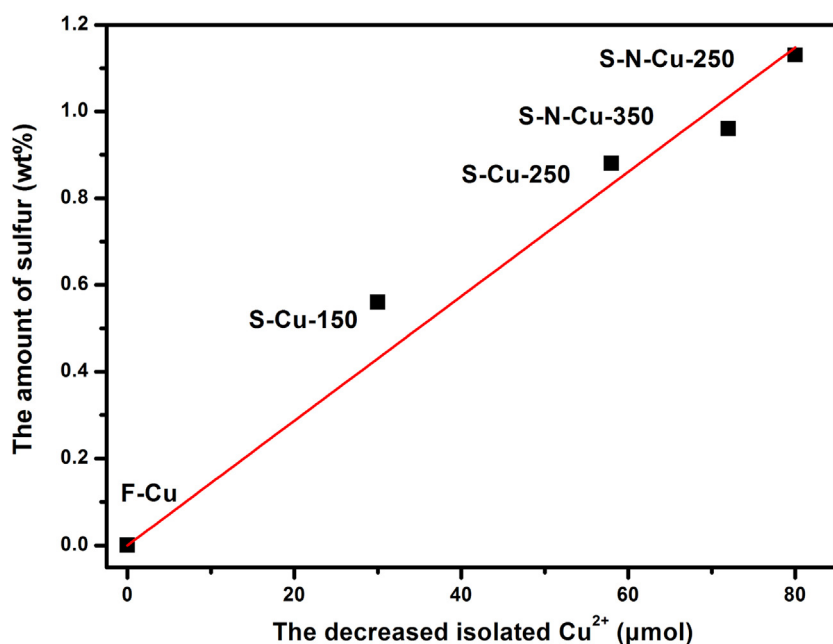
Fig. 10. The relationship between the decreased isolated Cu^{2+} and the mole of sulfur on catalysts.
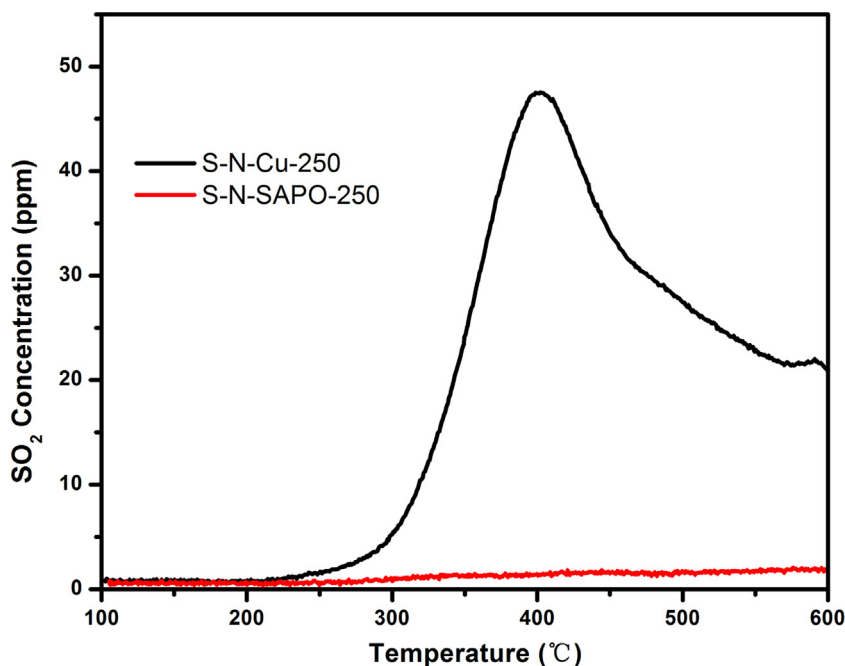

Fig. 11. TPD profiles of sulfated support and Cu/SAPO-34 catalyst.

TOFs of S-N-Cu-250 are the same as those of other sulfated catalysts. Thus, although ammonia sulfate species and copper sulfate decompose at different temperatures, their poison mechanism appear to be the same, i.e. by occupying the isolated Cu^{2+} sites. This is further supported by the directly correlation between the number of Cu^{2+} sites and the amount of sulfur as shown in Fig. 10.

Does the formation of sulfate species require the copper sites? This question can be answered by running a comparative experiment using HSAPO-34 (support) and a fresh Cu/SAPO-34 catalyst with both materials treated under identical conditions (S-N-SAPO-250 and S-N-Cu-250 in Table 1). The TPD results (Fig. 11) show no detectable SO_2 from S-N-SAPO-250. It is obvious that the formation of any sulfate species (ammonia sulfate species or copper sulfate)

does not take place in the gas phase and requires the presence of the copper sites. Copper ions in zeolites are known to be active centers for SO_2 oxidation to SO_3 [21]. SO_2 oxidation on a fresh Cu/SAPO-34 catalyst was also investigated in this work between room temperature and 500 °C. The SO_2 conversion, although low (<10%), monotonically increased with temperature (Fig. S8). Conceivably, forming a sulfate species or an adsorbed SO_3 molecule on the catalyst would be much easier than catalyzing the SO_2 oxidation to SO_3 because SO_3 desorption requires a significant activation energy. The adsorbed SO_3 on the copper sites can react with ammonia and water, forming ammonia sulfate species [22,23] under SCR conditions on Cu/SAPO-34.

Among all sulfated catalysts, S-N-Cu-250 deactivated the most because more isolated Cu^{2+} sites were occupied by ammonia sulfate species. However, the ammonia sulfate species formed on S-N-Cu-250 is easier to remove, which can be completely decomposed at 500 °C. On the other hand, copper sulfate formed on the other sulfated catalysts can only be partially removed at 600 °C.

5. Conclusions

The effect of sulfur on the NH_3-SCR activity over Cu/SAPO-34 was investigated under various sulfation conditions. Copper sulfate was formed on all sulfated catalysts. The higher the sulfation temperature (150–350 °C), the more copper sulfate formation. At 250 °C, ammonia inhibits the formation of copper sulfate because ammonia competes with SO_2 for the copper sites, forming ammonia sulfate species instead. Ammonia sulfate species was only found on Cu/SAPO-34 treated with both SO_2 and NH_3 at 250 °C. Both copper sulfate and ammonia sulfate species decrease the SCR reaction rate of the Cu/SAPO-34 catalysts by reducing the number of Cu^{2+} sites. The deactivation mechanism by these two types of sulfur species are the same. However, ammonia sulfate is easier to decompose than copper sulfate.

Acknowledgements

Appendix A. Supplementary data

Supplementary data associated with this article can be found, in the online version, at http://dx.doi.org/10.1016/j.apcatb.2016.11.033.

References

[1] Ja Hun Kwak, Russell G. Tonkyn, J. Catal. 275 (2010) 187.
[2] Junjie Xue, Xinquan Wang, Gong shin Qi, Jun Wang, Meiqing Shen, Wei Li, J. Catal. 297 (2013) 56.
[3] Dustin W. Fickel, Elizabeth D' Addio, Jochen A. Lauterbacha, Raul F. Lobo, Appl. Catal. B 102 (2011) 441.
[4] Di Wang, Li Zhang, Krishna Kamasamudram, S. William Epling, ACS Catal. 3 (2013) 871.
[5] J.C. Wang, Z.Q. Liu, G.F, L.P. Chang, W.R. Bao, Fuel 109 (2013) 101.
[6] Yisun Cheng, Clifford Montreuil, Giovanni Cavataio, Christine Lambert, SAE Paper 2008-01-1023, (2008).
[7] Yisun Cheng, Christine Lambert, Do Heui Kim, Ja Hun Kwak, Sung June Cho, Charles H.F. Peden, Catal. Today 151 (2010) 266.
[8] Meiqing Shen, Huaiyou Wen, Teng Hao, Tie Yu, Dequan Fan, Jun Wang, Wei Li, Jianqiang Wang, Catal Sci. Technol. 5 (2014) 1741.
[9] D. William Brookshear, Jeong-gil Nam, Ke Nguyen, Todd J. Toops, Andrew Binder, Catal. Today 258 (2015) 359.
[10] Kurnia Wijayanti, Stanislava Andonova, Ashok Kumar, Junhui Li, Krishna Kamasamudram, Neal W. Currier, Aleksey Yezerets, Louise Olsson, Appl. Catal. B 166 (2015) 568.
[11] Klaus Hjuler, Kim Dam-Johansen, Ind. Eng. Chem. Res. 31 (1992) 2110.
[12] H. Bai, P. Biswas, T. Keener, Ind Eng. Chem. Res 33 (1994) 1231.
[13] Sung-Won Ham, Hoon Choi, In-Sik Nam, Yong Gul Kim, Catal. Today (11 1992) 611.
[14] Sung-Won Ham, In-Sik Nam, Yong Gul Kim, Korean J. Chem. Eng. 17 (2000) 318.
[15] L. Zhang, Di Wang, Yong Liu, Krishna Kamasamudram, Junhui Li, William Epling, Appl. Catal. B 156 (2014) 371.
[16] Jun Wang, Dequan Fan, Tie Yu, Jianqiang Wang, Teng Hao, Xiaoqian Hu, Meiqing Shen, J. Catal. 322 (2015) 84.
[17] A. Buchholz, W. Wang, M. Xu, A. Arnold, M. Hunger, Micro. Meso. Mater. 56 (2002) 267.
[18] Lei Wang, Jason R. Gaudet, Wei Li, Duan Weng, J. Catal. 306 (2013) 68.
[19] Yuan Li, Meiqing Shen, Jun Wang, Taoming Wan, Jianqiang Wang, Catal. Sci. Technol. 5 (2015) 1731.
[20] Lei Wang, Wei Li, Gongshin Qi, Duan Weng, J. Catal. 289 (2012) 21.
[21] Sung-Won Ham, Hoon Choi, In-Sik Nam, Yong Gul Kim, Ind. Eng. Chem. Res. 34 (1995) 1616.
[22] M. Ziolek, I. Sobczak, I. Nowak, M. Daturi, J.C. Lavalley, Top. Catal. 11 (2000) 343.
[23] Jung Bin Lee, Seong Keun Kim, Dong Wha Kim, Ki Hyung Kim, Sung Nam Chun, Kwang Beom Hur, Sang Mun Jeong, Korean J. Chem. Eng. 29 (2012) 270.